Aptamer-Based Sensor Arrays for the Detection and Quantitation of Proteins

ARTICLE *in* ANALYTICAL CHEMISTRY · AUGUST 2004

Impact Factor: 5.64 · DOI: 10.1021/ac049858n · Source: PubMed

8 AUTHORS, INCLUDING:

Eun jeong Cho
University of Texas at Austin
26 PUBLICATIONS **1,377** CITATIONS
SEE PROFILE

D.P. Neikirk
University of Texas at Austin
226 PUBLICATIONS **2,597** CITATIONS
SEE PROFILE

John Thomas McDevitt
New York University
204 PUBLICATIONS **3,992** CITATIONS
SEE PROFILE

Anal. Chem. **2004,** *76,* 4066−4075

Aptamer-Based Sensor Arrays for the Detection and Quantitation of Proteins

Romy Kirby,† Eun Jeong Cho,† Brian Gehrke,† Travis Bayer,† Yoon Sok Park,‡ Dean P. Neikirk,‡ John T. McDevitt,† and Andrew D. Ellington*,†

Department of Chemistry and Biochemistry, Department of Electrical & Computer Engineering, and Institute for Cell and Molecular Biology, University of Texas at Austin, Austin, Texas 78712

Aptamer biosensors have been immobilized on beads, introduced into micromachined chips on the electronic tongue sensor array, and used for the detection and quantitation of proteins. Aptamer chips could detect proteins in both capture and sandwich assay formats. Unlike most protein-based arrays, the aptamer chips could be stripped and reused multiple times. The aptamer chips proved to be useful for screening aptamers from in vitro selection experiments and for sensitively quantitating the biothreat agent ricin.

Aptamers are functional binding species that have been selected from combinatorial oligonucleotide libraries by in vitro selection.[1,2] To date, numerous aptamers with high affinity and selectivity have been created against a variety of targets, such as small organics, peptides, proteins, and even whole cells.[3,4] Aptamers can compete with antibodies in a number of analytical applications, such as ELISA-like assays,[5] flow cytometry,[6,7] affinity probe capillary electrophoresis,[8] capillary electrochromatography,[9,10] affinity chromatography,[11,12] in high-throughput screening assays,[13] and more generally as biosensors, including in arrays.[14−20] Aptamers have several advantages over traditional antibody-based reagents. Unlike antibodies, which are generally produced in organisms, aptamers can be chemically synthesized, and therefore specifically labeled with radioscopic, fluorescent, or other reporters.[21] Moreover, while many antibodies are temperature-sensitive and can denature upon contact with surfaces, leading to limited shelf lives and possible compromise of assay integrity, aptamers are stable to long-term storage, can be transported at ambient temperature, and undergo reversible denaturation.

Because of these advantages, it would be extremely useful to make aptamer arrays. This is especially true because in recent years, high-density DNA microarrays have proved to be powerful tools for genetic analyses and diagnostic assays.[22−24] Since aptamers are nucleic acids, experience with DNA arrays should be applicable to the development of aptamer arrays. In turn, aptamer arrays can potentially expand the scope of DNA microarrays to recognize expressed proteins as well as expressed mRNAs. In this regard, numerous aptamers have already been selected against a wide array of proteins, and the possibility of acquiring aptamers against proteomes has been advanced by automation of the in vitro selection procedure.[25]

The nature of the platform that will be used for the generation of aptamer arrays is open to question. Simply printing aptamers on polylysine-coated slides is unlikely to be successful, as the aptamers will denature upon electrostatic capture. Walt and coworkers have adapted aptamers to high-density fiber-optic arrays.[18] Stanton and researchers at the company Archemix have generated a small aptamer array that relies on scanning fluorescence anisotropy measurements.[19]

We wanted to integrate aptamer arrays with a device that could also deliver samples and perform complex assay procedures. In recent years, a chip-based microsphere array (or "electronic taste chip")[26] has been developed for the digital analysis of complex fluids. This platform relies on micromachined wells that contain microspheres with immobilized receptors and thus should allow

* Corresponding author. Phone: 512-232-3424. Fax: 512-471-7014. E-mail: andy.ellington@mail.utexas.edu.

† Department of Chemistry and Biochemistry and Institute for Cell and Molecular Biology.

‡ Department of Electrical & Computer Engineering.

(1) Ellington, A. D.; Szostak, J. W. *Nature* **1990**, *346*, 818−822.
(2) Tuerk, C.; Gold, L. *Science* **1990**, *249*, 505−510.
(3) Wilson, D. S.; Szostak, J. W. *Annu. Rev. Biochem.* **1999**, *68*, 611−647.
(4) Famulok, M.; Mayer, G.; Blind, M. *Acc. Chem. Res.* **2000**, *33*, 591−599.
(5) Drolet, D. W.; Moon-McDermott, L.; Romig, T. S. *Nat. Biotechnol.* **1996**, *14*, 1021−1025.
(6) Davis, K. A.; Abrams, B.; Lin, Y.; Jayasena, S. D. *Nucleic Acids Res.* **1996**, *24*, 702−706.
(7) Davis, K. A.; Lin, Y.; Abrams, B.; Jayasena, S. D. *Nucleic Acids Res.* **1998**, *26*, 3915−3924.
(8) German, I.; Buchanan, D. D.; Kennedy, R. T. *Anal. Chem.* **1998**, *70*, 4540−4545.
(9) Kotia, R. B.; Li, L.; McGown, L. B. *Anal. Chem.* **2000**, *72*, 827−831.
(10) Rehder, M. A.; McGown, L. B. *Electrophoresis* **2001**, *22*, 3759−3764.
(11) Romig, T. S.; Bell, C.; Drolet, D. W. *J. Chromatogr., B: Biomed. Sci. Appl.* **1999**, *731*, 275−284.
(12) Deng, Q.; German, I.; Buchanan, D.; Kennedy, R. T. *Anal. Chem.* **2001**, *73*, 5415−5421.
(13) Green, L. S.; Bell, C.; Janjic, N. *Biotechniques* **2001**, *30*, 1094−1096, 1098, 1100 passim.
(14) Kleinjung, F.; Klussmann, S.; Erdmann, V. A.; Scheller, F. W.; Fuerste, J. P.; Bier, F. F. *Anal. Chem.* **1998**, *70*, 328−331.
(15) Potyrailo, R. A.; Conrad, R. C.; Ellington, A. D.; Hieftje, G. M. *Anal. Chem.* **1998**, *70*, 3419−3425.
(16) Liss, M.; Petersen, B.; Wolf, H.; Prohaska, E. *Anal. Chem* **2002**, *74*, 4488−4495.
(17) Spiridonova, V. A.; Kopylov, A. M. *Biochemistry (Moscow)* **2002**, *67*, 706−709.
(18) Lee, M.; Walt, D. R. *Anal. Biochem.* **2000**, *282*, 142−146.
(19) McCauley, T. G.; Hamaguchi, N.; Stanton, M. *Anal. Biochem.* **2003**, *319*, 244−250.
(20) Rajendran, M.; Ellington, A. D. *Opt. Biosens.* **2002**, 369−396.
(21) Jayasena, S. D. *Clin. Chem.* **1999**, *45*, 1628−1650.
(22) Lockhart, D. J.; Winzeler, E. A. *Nature* **2000**, *405*, 827−836.
(23) Brown, P. O.; Botstein, D. *Nat. Genet.* **1999**, *21*, 33−37.
(24) Walt, D. R. *Science* **2000**, *287*, 451−452.
(25) Cox, J. C.; Rudolph, P.; Ellington, A. D. *Biotechnol. Prog.* **1998**, *14*, 845−850.

10.1021/ac049858n CCC: $27.50
Published on Web 05/25/2004

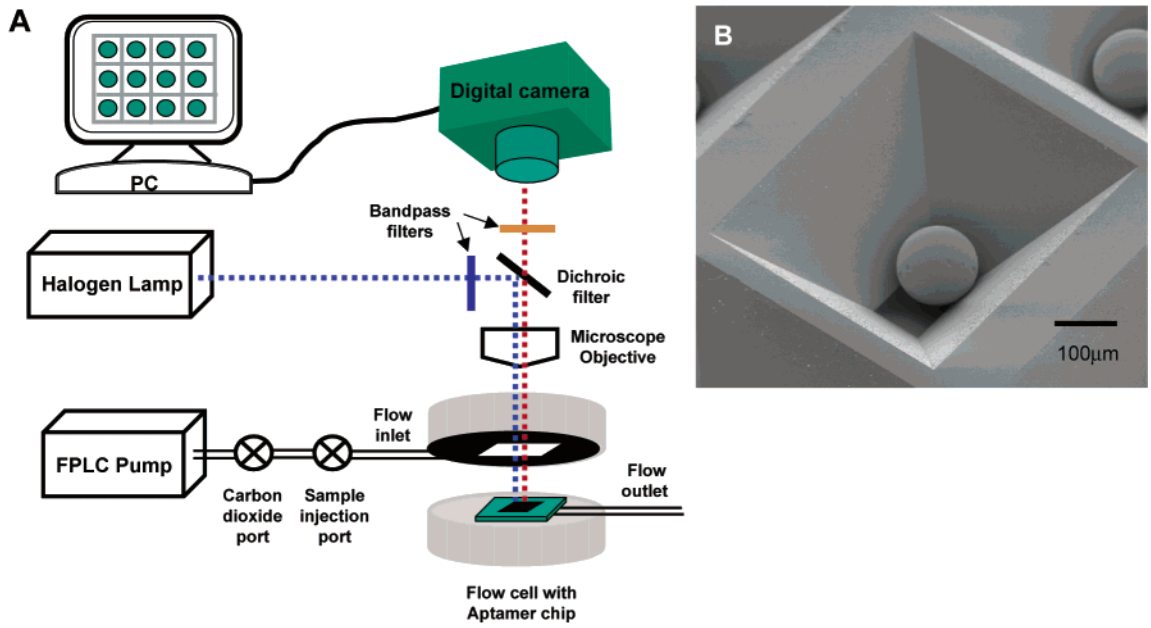

Figure 1. Detection system. (A) The electronic tongue setup contains a fluid delivery system, fluorescence microscope, digital camera, flow cell in which the aptamer chip will be loaded, and computer for data analysis. (B) Close-up look at a bead in a rectangular-shaped micromachined well of the aptamer chip.

the development of sandwich assays. This so-called "electronic taste chip" has demonstrated its analytical potential in detecting a variety of analyte classes (acids, metal cations, metabolic cofactors, sugars, and proteins) in complex, homogeneous solution.[26−31] More importantly, the chip-based microsphere array has proven useful for the rapid and specific detection of nucleic acid sequences.[32] Therefore, we attempted to adapt the microsphere array to aptamer receptors. A unique method for the facile immobilization of aptamers was developed and proved to be immediately useful for screening aptamer libraries. Aptamer receptors could be used for the quantitation of protein targets and for the development of sandwich assays, including the quantitation of unlabeled ricin. Surprisingly, unlike most protein biosensors, the aptamer biosensors could be denatured and reused many times on the same chip, without loss of function.

EXPERIMENTAL SECTION

Detection System. The "electronic tongue" (ET)[26] developed by the McDevitt lab at the University of Texas at Austin consists of a flow cell connected to an FPLC (fast performance liquid chromatograph) pump for sample introduction and a fluorescence microscope for observation (Figure 1A). In more detail, the individual components included an Amersham Pharmacia Biotech P900 pump with carbon dioxide and sample injection ports added downstream of the pump (three-way stopcock; Baxter, Deerfield, IL); a Zeiss Axioplan2 compound microscope (5× objective) with a fluorescence unit containing band-pass filters for Alexa-Fluor$_{488}$ (λ_{ex} 480/40 nm, λ_{em} 535/50 nm) and Cy3 (λ_{ex} 545/30 nm, λ_{em} 610/75 nm) and dichroic filters (Alexa-Fluor$_{488}$ λ 505 nm LP and Cy3 λ 570 nm LP), and a Hamamatsu C4742-95 b/w digital camera. The heart of the system was the flow cell, which consisted of a circular metal housing (3.5 cm diameter), top and bottom lenses (3 cm diameter), and an etched silicon chip that could be inserted into the housing (1.2 cm × 1.2 cm). Captured images were analyzed using image analysis software (IP Lab 3.6.3, Scanalytics, Inc., Fairfax, VA).

Aptamers were biotinylated at their 5′ ends during transcription by introducing a biotin-GpG dinucleotide into the reaction mixture. Biotin-GpG was synthesized utilizing standard RNA phosphoramidite chemistry (dmf-G-RNA-CPG, *i*-Pr-Pac-G-CE phosphoramidite, and 5′-biotin phosphoramidite were purchased from Glen Research, Sterling, VA). Deprotected biotin-GpG was purified on a Poly-Pak column (Glen Research, Sterling, VA) following the manufacturer's protocol. A 20 µL transcription reaction typically contained 800 ng of template DNA, 30 mM DTT, 5 mM ATP, 5 mM CTP, 5 mM UTP, 2 mM GTP, 3 mM biotin-GpG, and 2 units of T7 RNA polymerase (Epicentre, Madison, WI) in transcription buffer (60 mM Tris·Cl pH 8.0, 10 mM NaCl, 40 mM $MgCl_2$, 6.8 mM spermidine). Transcription reactions were incubated at 37 °C for 4 h. The transcription reactions were then treated with 1 µL of RNase-free DNase (Epicentre, Madison, WI) for 15 min at 37 °C, purified on an 8% denaturing acrylamide gel, and ethanol-precipitated. The purified, biotinylated aptamers were resuspended in water and stored at −20 °C.

All of the anti-lysozyme, anti-ricin aptamers, and the anti-Rev aptamer used in the current studies have previously been described[33−35] with three exceptions. The anti-lysozyme aptamers E, J, and M were selected from a random sequence library by

(26) Goodey, A.; Lavigne, J. J.; Savoy, S. M.; Rodriguez, M. D.; Curey, T.; Tsao, A.; Simmons, G.; Wright, J.; Yoo, S. J.; Sohn, Y.; Anslyn, E. V.; Shear, J. B.; Neikirk, D. P.; McDevitt, J. T. *J. Am. Chem. Soc.* **2001**, *123*, 2559−2570.
(27) Christodoulides, N.; Tran, M.; Floriano, P. N.; Rodriguez, M.; Goodey, A.; Ali, M.; Neikirk, D.; McDevitt, J. T. *Anal. Chem.* **2002**, *74*, 3030−3036.
(28) Curey, T. E.; Goodey, A.; Tsao, A.; Lavigne, J.; Sohn, Y.; McDevitt, J. T.; Anslyn, E. V.; Neikirk, D.; Shear, J. B. *Anal. Biochem.* **2001**, *293*, 178−184.
(29) Curey, T. E.; Salazar, M. A.; Oliveira, P.; Javier, J.; Dennis, P. J.; Rao, P.; Shear, J. B. *Anal. Biochem.* **2002**, *303*, 42−48.
(30) Goodey, A. P.; McDevitt, J. T. *J. Am. Chem. Soc.* **2003**, *125*, 2870−2871.
(31) McCleskey, S. C.; Griffin, M. J.; Schneider, S. E.; McDevitt, J. T.; Anslyn, E. V. *J. Am. Chem. Soc.* **2003**, *125*, 1114−1115.
(32) Ali, M. F.; Kirby, R.; Goodey, A. P.; Rodriguez, M. D.; Ellington, A. D.; Neikirk, D. P.; McDevitt, J. T. *Anal. Chem.* **2003**, *75*, 4732−4739.

Table 1. Sequences of Anti-Protein Aptamers

aptamers		sequences
anti-lysozyme aptamers	clone 1	5′GGGAATGGATCCACATCTACGAATTCATCAGGGCTAAAGAG TGCAGAGTTACTTAGTTCACTGCAGACTTGACGAAGCTT
	clone 2	5′GGGAATGGATCCACATCTACGAATTCGGTGATCATGGCAGT GTACGCGGGCGGACATTCACTGCAGACTTGACGAAGCTT
	clone 3	5′GGGAATGGATCCACATCTACGAATTCGGTTGTGAAGATTGG GAGCGTCGTGGCTACTTCACTGCAGACTTGACGAAGCTT
	clone 4	5′GGGAATGGATCCACATCTACGAATTCGTAAATCGTCGACAG GAATTGGCGGGCCGGTTCACTGCAGACTTGACGAAGCTT
	clone 5	5′GGGAATGGATCCACATCTACGAATTCGAATTGCGACAGTCG GGACATGTCGCGAGGTTCACTGCAGACTTGACGAAGCTT
	clone 6	5′GGGAATGGATCCACATCTACGAATTCGGAATGAGTGCCCTG CAAGCGAGGGCTAGCTTCACTGCAGACTTGACGAAGCTT
	clone E	5′GGGAAUGGAUCCACAUCUACGAAUUCGGAACCCGCUAGGA GUGAAACGGGGCGUGCUUCACUGCAGACUUGACGAAGCUU
	clone J	5′GGGAAUGGAUCCACAUCUACGAAUUCGUUGGAGAAUAUUA GCGCUACAGAACAGGUUCACUGCAGACUUGACGAAGCUU
	clone M	5′GGGAAUGGAUCCACAUCUACGAAUUCGGAAAUUGGGGUUA UUGUUGCAACGGACGGUUCACUGCAGACUUGACGAAGCUU
anti-ricin aptamer		5′GGCGAAUUCAGGGGACGUAGCAAUGACUGCC
anti-Rev aptamer		5′GGGAATGGATCCACATCTACGAATTCGTTGGAAGAGAGGAA AATTGACAGCGCGACTTCACTGCAGACTTGACGAAGCT

methods similar to those described by Cox et.al.[34] The aptamer sequences are summarized in Table 1.

Relative Affinity and Reactivity Studies of Anti-Lysozyme Aptamer Clones. Nine different anti-lysozyme aptamer clones, from selections done in our lab, were biotinylated and immobilized onto streptavidin agarose beads (Sigma, St. Louis, MO). For each of the clones, 10 μL of the streptavidin agarose bead suspension was washed with 500 μL of Tris buffer (20 mM Tris pH 7.6, 100 mM NaCl, 5 mM $MgCl_2$) three times and resuspended in 40 μL of Tris buffer. Biotinylated anti-lysozyme aptamer (600 pmol) was resuspended in 40 μL of Tris buffer, heat-denatured for 3 min at 70 °C, and allowed to cool to room temperature. The heat-denatured biotinylated anti-lysozyme aptamer was mixed with the washed streptavidin agarose beads and allowed to rotate for 30 min. The newly conjugated anti-lysozyme aptamer beads were washed with 200 μL of Tris buffer three times, resuspended in 600 μL of Tris buffer, and stored at 4 °C. Lysozyme (Sigma, St. Louis, MO) was labeled with Cy3 following the protocol from a Cy3 monoreactive dye pack (Amersham Biosciences, Piscataway, NJ).

Initial experiments were done to gauge the relative affinities of the anti-lysozyme aptamer clones. A small aliquot of each of the anti-lysozyme aptamer clone beads was removed, and the beads were loaded into the wells of a 4 × 3 silicon chip. Negative control beads (anti-Rev aptamer, pool RNA, and unmodified streptavidin agarose beads) were also loaded on the chip. The loaded chip was enclosed in the flow cell device.

The loaded flow cell was washed with Tris buffer supplied through the fluidic pump. All additions of elution buffer (100 mM sodium citrate, 10 mM EDTA, 7 M urea, pH 5.0) and Cy3-labeled lysozyme were made through an injection port inserted directly upstream of the inlet to the flow cell. The assay was broken into four steps: (1) The beads were washed with 1 mL of elution buffer, followed by a subsequent reintroduction of Tris buffer. (2) Cy3-labeled lysozyme (1.8 μg/mL, 100 μL) was injected into the system and allowed to incubate for 2 min with the anti-lysozyme aptamer beads. (3) The beads were washed with Tris buffer at a flow rate of 0.1 mL/min for 4 min to wash away any unbound Cy3-labeled lysozyme. (4) An image was captured showing the beads' response. Fluorescence intensity data were collected for each anti-lysozyme aptamer clone, corrected by subtraction of the intensity recorded from the negative control bead, and graphed.

Subsequent experiments were performed with anti-lysozyme aptamer clones 1, 3, and 6. A small aliquot of beads from each clone type was removed and loaded into the wells of a 4 × 3 silicon chip. Negative control beads (RNA pool) were also loaded on the chip. The loaded chip was enclosed in the flow cell device.

The loaded flow cell was washed with Tris buffer supplied through the fluidic pump. All additions of elution buffer and Cy3-labeled lysozyme were made through an injection port inserted directly upstream of the inlet to the flow cell. The assay was broken into five steps: (1) The beads were washed with 1 mL of elution buffer, followed by a subsequent reintroduction of Tris buffer. (2) Cy3-labeled lysozyme (1.44 μg/mL, 100 μL) was injected into the system and allowed to incubate for 2 min with the anti-lysozyme aptamer beads. (3) The beads were washed with Tris buffer at a flow rate of 0.4 mL/min for 28 min to wash away any unbound Cy3-labeled lysozyme. Images were captured at six different intervals. (4) The beads were washed again with 1 mL of elution buffer to remove the bound Cy3-labeled lysozyme and regenerate the anti-lysozyme aptamers, followed by a reintroduction of Tris buffer. An image was captured. (5) Cy3-labeled lysozyme (1.44 μg/mL, 100 μL) was reintroduced into the system and allowed to incubate for 2 min with the anti-lysozyme aptamer beads before they were washed with Tris buffer. A final image was captured. Fluorescence intensity data were collected for each anti-lysozyme aptamer clone, corrected by subtraction of the intensity of the negative control bead, and graphed as a function of time.

Anti-Ricin Aptamer Detection. Biotinylated anti-ricin aptamers were immobilized onto streptavidin agarose beads. A 10 μL volume of a streptavidin agarose bead suspension was washed

(33) Giver, L.; Bartel, D. P.; Zapp, M. L.; Green, M. R.; Ellington, A. D. *Gene* **1993**, *137*, 19−24.
(34) Cox, J. C.; Ellington, A. D. *Bioorg. Med. Chem.* **2001**, *9*, 2525−2531.
(35) Hesselberth, J. R.; Miller, D.; Robertus, J.; Ellington, A. D. *J. Biol. Chem.* **2000**, *275*, 4937−4942.

three times with 500 μL of PBSM buffer (PBS, 5 mM $MgCl_2$) and resuspended in 40 μL of PBSM buffer. Biotinylated anti-ricin aptamer (600 pmol) was resuspended in 40 μL of PBSM buffer, heat-denatured for 3 min at 70 °C, and allowed to cool to room temperature. The heat-denatured, biotinylated anti-ricin aptamer was mixed with the washed streptavidin agarose beads and gently rotated for 30 min. The conjugated anti-ricin aptamer beads were washed with 200 μL of PBSM buffer three times, resuspended in 600 μL of PBSM buffer, and stored at 4 °C. Ricin A chain (Sigma, St. Louis, MO) was labeled with Alexa-Fluor$_{488}$ according to the protocol supplied with Alexa-Fluor$_{488}$ maleimide (Molecular Probes, Eugene, OR). Alexa-Fluor$_{488}$-labeled ricin was stored at 4 °C.

A small aliquot of anti-ricin aptamer beads was removed from the stock solution, and three individual beads were loaded into the wells of a 3 × 2 silicon chip. Three negative control beads (streptavidin agarose beads) were also loaded on the chip. The loaded chip was enclosed in the flow cell device. Carbon dioxide was used to displace the air in the loaded flow cell prior to the initial introduction of PBSM buffer via the FPLC pump. The beads were then washed with 1 mL of elution buffer, followed by a reintroduction of PBSM buffer. All additions of elution buffer and Alexa-Fluor$_{488}$-labeled ricin were made through an injection port which was inserted directly upstream of the inlet to the flow cell. Binding assays were typically broken into three steps: (1) Ricin in PBSM was injected (8 μg/mL, 400 μL Alexa-Fluor$_{488}$-labeled ricin) and allowed to flow over the anti-ricin aptamer beads. (2) The beads were washed with PBSM buffer at a flow rate of 0.1 mL/min for 4 min, followed by a flow rate of 0.5 mL/min for 30 s, to wash away any unbound Alexa-Fluor$_{488}$-labeled ricin. (3) An image was captured showing the aptamer beads' response to the addition of the ricin in PBSM. Steps 1−3 were repeated for nine more additions of ricin in PBSM (each sample was 8 μg/mL, 400 μL of Alexa-Fluor$_{488}$-labeled ricin solution) in order to explore the cumulative effects of serial injections of target. Fluorescence intensity data were collected from the images, corrected by subtraction of the intensity of the negative control bead, and graphed against the concentration of Alexa-Fluor$_{488}$-labeled ricin.

Aptamer−Antibody Sandwich Assay. An anti-ricin antibody (anti-lectin, *Ricinus communis* (RCA_{II}), Sigma, St. Louis, MO) was labeled with Alexa-Fluor$_{488}$ following the protocol provided with an Alexa-Fluor$_{488}$ NHS protein-labeling kit (Molecular Probes, Eugene, OR). A small aliquot of anti-ricin aptamer beads was removed from the stock solution, and the beads were loaded into the wells of five 3 × 2 silicon chips. Negative control beads (containing biotinylated RNA pool) were also loaded on the chip. The loaded chip was enclosed in the flow cell device and washed with PBSM buffer supplied through the FPLC pump. All subsequent additions of solutions were made through an injection port inserted directly upstream of the inlet to the flow cell. The assay was broken into five steps: (1) The beads were washed with 1 mL of elution buffer, followed by a reintroduction of PBSM buffer (1 mL). (2) Ricin in PBSM (3.5 μg/mL, 100 μL) was injected into the system and incubated for 5 min with the anti-ricin aptamer beads. (3) The beads were washed with 1 mL of PBSM buffer to wash away any unbound ricin. (4) Alexa-Fluor$_{488}$-labeled anti-ricin antibody in PBSM (53 μg/mL, 100 μL) was injected into the system and incubated for 10 min with the anti-ricin aptamer beads. (5) The beads were washed with 1 mL of PBSM buffer to wash away any unbound Alexa-Fluor$_{488}$-labeled anti-ricin antibody. An image was captured showing the beads' response. The chip was removed from the flow cell, and a new one was inserted. Steps 1−5 were repeated using progressively lower concentrations of ricin and Alexa-Fluor$_{488}$-labeled anti-ricin antibody in PBSM: chip 2, ricin (2.24 μg/mL, 100 μL) and Alexa-Fluor$_{488}$-labeled anti-ricin antibody (33.6 μg/mL, 100 μL); chip 3, ricin (0.96 μg/mL, 100 μL) and Alexa-Fluor$_{488}$-labeled anti-ricin antibody (14.4 μg/mL, 100 μL); chip 4, ricin (0.32 μg/mL, 100 μL) and Alexa-Fluor$_{488}$-labeled anti-ricin antibody (4.8 μg/mL, 100 μL). Fluorescence intensity data were collected from the images, corrected by subtraction of the intensity of the negative control bead, and graphed against the concentration of injected ricin.

Assaying Aptamer Selectivity. Anti-ricin aptamer on beads or anti-lysozyme aptamer on beads (clone 1) was denatured with the elution buffer. The aptamer beads were washed three times with 500 μL of elution buffer, followed by a reintroduction of the appropriate buffer (500 μL of PBSM three times for anti-ricin aptamer beads and 500 μL of Tris buffer three times for anti-lysozyme aptamer beads; each individual wash step took 2 min). The beads (three per each aptamer) were loaded into the wells of the 3 × 2 silicon chip. The loaded chip was enclosed in the flow cell device. Carbon dioxide was used to displace the air in the loaded flow cell prior to the initial buffer introduction. PBSM buffer (supplied by an FPLC pump) was then introduced into the loaded flow cell.

Two stock solutions of Alexa-Fluor$_{488}$-labeled proteins were made. Ricin (Sigma, St. Louis, MO) and lysozyme (Sigma, St. Louis, MO) were labeled with Alexa-Fluor following the protocols from Alexa-Fluor$_{488}$-labeling kits. The Alexa-Fluor$_{488}$-labeled proteins were stored at 4 °C.

The loaded flow cell was washed with 1 mL of elution buffer, followed by a reintroduction of PBSM buffer. A background image was captured after washing with 1 mL of PBSM (0.1 mL/min). Wash cycles with PBSM were introduced through the FPLC pump. All additions of elution buffer and Alexa-Fluor$_{488}$-labeled ricin and lysozyme were made through an injection port inserted directly upstream of the inlet to the flow cell. The assay was broken into seven steps: (1) Alexa-Fluor$_{488}$-labeled ricin was injected (24 μg/mL, 400 μL) and allowed to flow over the anti-ricin and anti-lysozyme aptamer beads for 1 min. (2) The beads were washed with PBSM buffer at a flow rate of 0.1 mL/min for 10 min to wash away any unbound Alexa-Fluor$_{488}$-labeled ricin. Images were captured every 2 min during the wash cycle to show the beads' response to the addition of Alexa-Fluor$_{488}$-labeled ricin. (3) Elution buffer (5 mL) was injected into the flow cell to denature the aptamers and elute all of the bound Alexa-Fluor$_{488}$-labeled ricin. An image was captured to show that the Alexa-Fluor$_{488}$-labeled ricin had been removed and that the aptamer beads exhibited a signal comparable to the initial background signal. (4) PBSM buffer was reintroduced into the flow cell. (5) Alexa-Fluor$_{488}$-labeled lysozyme was injected (10.8 μg/mL, 400 μL) and allowed to flow over the anti-ricin and anti-lysozyme aptamer beads for 1 min. (6) The beads were washed with PBSM buffer at a flow rate of 0.1 mL/minute for 10 min to wash away any unbound Alexa-Fluor$_{488}$-labeled lysozyme. Images were captured every 2 min during the wash cycle to show the beads' response to the addition of Alexa-Fluor$_{488}$-labeled lysozyme. (7) Elution buffer (5 mL) was injected into the flow cell to denature the aptamers and elute all of the bound Alexa-Fluor$_{488}$-labeled lysozyme. An image was

captured to show that the Alexa-Fluor$_{488}$-labeled lysozyme had been removed and that the aptamer beads exhibited a signal comparable to the initial background signal. Fluorescence intensity data were collected from the images and graphed against time.

Aptamer Regeneration. In initial regeneration assays, anti-ricin aptamer beads (400 pmol) were separated into four tubes. The anti-ricin aptamer beads were then either used as is, heat-denatured (3 min at 70 °C), washed with an elution buffer (100 mM sodium citrate, 10 mM EDTA, 7 M urea, pH 5.0), or heat-denatured and washed with an elution buffer. All beads were then incubated with Alexa-Fluor$_{488}$-labeled ricin (128 μg/mL, 25 μL) and washed with 200 μL of PBSM three times to remove any unbound Alexa-Fluor$_{488}$-labeled ricin. Fluorescence intensity data were collected by fluorescence microscopy.

Regeneration experiments were also carried out on the ET with both anti-ricin aptamer beads and pool RNA beads. Anti-ricin aptamer beads (400 μL) and pool RNA beads (100 μL) were washed with 500 μL of elution buffer two times (rotating 2 min for the first wash), followed by a reintroduction of PBSM buffer (500 μL two times; rotating 2 min for the first wash), and a final resuspension in 100 μL of PBSM buffer. A total of 5 μL was removed from each tube for the background fluorescent measurements of unexposed anti-ricin aptamer beads and pool RNA beads. Alexa-Fluor$_{488}$-labeled ricin (128 μg/mL, 50 μL) was incubated with each tube of beads for 2 min (first protein incubation). Unbound Alexa-Fluor$_{488}$-labeled ricin was washed away with 500 μL of PBSM buffer two times. The washed beads were denatured with 500 μL of elution buffer two times and reintroduced to PBSM buffer (500 μL two times, rotating 2 min for the first wash). The anti-ricin aptamer beads were put through five more cycles of protein introduction, followed by elution buffer washes. Pool RNA beads were subject to two more cycles of protein introduction and elution wash. Images were captured after each protein incubation, as well as each elution wash. The fluorescence intensity of anti-ricin aptamer beads and pool RNA beads was graphed for each step.

RESULTS AND DISCUSSION

Description of the Electronic Tongue Sensor Array. The ET sensor array has previously been used to monitor the performance of a variety of chemical and biological sensors, including chemical sensors and antibodies.[26−32] The heart of the ET is a flow cell that contains a silicon chip with multiple, micromachined, pyramidal wells through which fluid can pass; the flow cell is integrated with a fluid delivery system for sample introduction (Figure 1A). A 4 × 3 or a 3 × 2 array was typically used in our experiments; however, somewhat larger arrays (10 × 10) have also been manufactured. Beads containing sensor elements are nestled into each well. The flow cell delivers solutions and analytes to the "top" of the chip, where the apertures of the wells are widest. The solute must then pass by each bead before exiting through the smaller apertures on the "bottom" of the chip. The ease with which aptamers can be generated and modified for immobilization made their adaptation to the device very desirable.

In order to better accommodate aptamer biosensors, modifications were introduced into the basic configuration of the ET. A carbon dioxide port (3-way valve) was added to the inlet tube (Figure 1A). Carbon dioxide was used to displace the air in the loaded flow cell prior to the initial buffer introduction. This innovation greatly reduced bubble formation and capture in the flow cell, a problem that had sometimes hampered data acquisition and that had previously limited the utility of the device for high-throughput applications. Carbon dioxide was chosen because of its high solubility in aqueous solutions.

In addition, the path length that was to be traversed by sample solutions introduced into the device via the FPLC pump was decreased by introducing a sample injection port (3-way valve) onto the inlet tube, immediately upstream of the flow cell (Figure 1A). This innovation substantially reduced the dilution of samples during their transit to the flow cell.

Engineering Aptamer Bead Sensor Elements for the Electronic Tongue. While chemical and biological sensors other than aptamers have previously been adapted to the ET, intensive engineering efforts were required for the introduction of each new sensor element. For example, in order to utilize chemical sensors the initial synthetic reactions had to plan for linkers that could be conjugated to beads, or else the sensor had to be further modified following synthesis. Biosensors, such as antibodies, could be generated more quickly and in parallel, but their immobilization on beads relied on relatively nondirected conjugation chemistries to any of a number of surface amines, frequently resulting in loss of function and requiring the optimization of both immobilization and analytical protocols.

Because aptamers are generated in vitro, their synthesis can potentially be modified to accommodate both immobilization and sensing. To this end, we have site-specifically introduced a single, 5′ terminal biotin during transcription. The compound biotin-GpG was used as an initiator for T7 RNA polymerase[36−38] transcription (but cannot be internally incorporated during transcription). While previous reports have shown that a relatively small number of RNA species can be initiated with biotinylated nucleotides,[39] we have now used this technique with literally hundreds of different constructs and have typically observed biotinylation yields of 40% (data not shown). Alternatively, biotinylated DNA aptamers could be chemically synthesized with a terminal biotin residue, or amplified using a primer that contained a biotin conjugate.

Commercially available streptavidin agarose beads (approximately 60−100 μm in diameter) were incubated with the biotinylated aptamers to produce aptamer−bead sensor elements. The use of streptavidin agarose beads obviated an avidin conjugation step that was used in previous bead-preparation protocols[26−31] and further decreased the time required to prepare individual chips for assay. The beads bound 50 pmol of biotin per μL of bead suspension and were incubated with a 20% excess of biotinylated aptamer for 30 min to fully saturate the binding sites (and thus minimize any variance in signal due to beads size). Any collected signals were eventually normalized relative to the size of the beads, and in fact, the standard deviation of signal was less than 12.5% in all experiments, irrespective of bead size. However, since the streptavidin agarose beads were much smaller than the beads that were previously used (120−350 μm), the dimensions of the silicon chip had to be altered so that the beads would not fall through the wells. The well dimensions that ultimately proved to be optimal

(36) Cheetham, G. M.; Jeruzalmi, D.; Steitz, T. A. *Nature* **1999**, *399*, 80−83.
(37) Bandwar, R. P.; Jia, Y.; Stano, N. M.; Patel, S. S. *Biochemistry* **2002**, *41*, 3586−3595.
(38) Kuzmine, I.; Gottlieb, P. A.; Martin, C. T. *J. Biol. Chem.* **2003**, *278*, 2819−2823.
(39) Pitulle, C.; Kleineidam, R. G.; Sproat, B.; Krupp, G. *Gene* **1992**, *112*, 101−105.

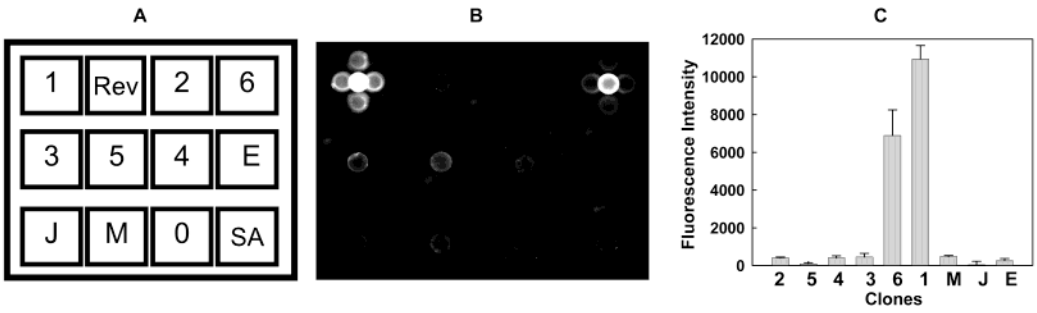

Figure 2. Parallel screening of anti-lysozyme aptamer clones. (A) Position of anti-lysozyme aptamer clones (1−6, E, J, and M) and three negative control beads in in a 3 × 4 chip. The negative controls were an anti-Rev aptamer (Rev), pool RNA (0), and unmodified streptavidin agarose beads (SA). (B) Fluorescent images of the anti-lysozyme aptamers and controls responding to Cy3-labeled lysozyme. (C) Fluorescence intensities of Cy3-labeled lysozyme captured by different anti-lysozyme aptamer clones.

were 70 μm × 140 μm (Figure 1B).

The use of rectangular rather than square wells was also an innovation. Square wells tended to be completely blocked by some beads, leading to a reduction in flow and a concomitant buildup of pressure within the system, sometimes resulting in cracking of the silicon chip. Rectangular wells always allowed solution to flow around individual beads. Nonetheless, fluid flow through the porous beads and past the aptamer biosensors in rectangular wells was more than sufficient for analyte detection, as will be seen below.

Overall, one of the advantages of loading biotinylated aptamers directly onto preconjugated streptavidin beads was that multiple different biosensors could be processed in parallel and chips could be quickly prepared. The total time for the construction of a 4 × 3 aptamer array was typically 8 h (6 h for aptamer transcription and purification, 45 min for bead conjugation, and 20−40 min for bead loading). Multiple chips were prepared in parallel, and only the time required for bead loading was extended.

Using the Electronic Tongue To Assess in Vitro Selection Experiments. The facile loading of aptamer biosensors onto the electronic tongue immediately suggested a practical application for this platform. An in vitro selection experiment typically yields a number of aptamers or aptamer families (a series of related aptamers). While these aptamers as a whole represent the tightest-binding species in a nucleic acid population, each selected sequence must nonetheless still be screened for its relative ability to bind to a target ligand. Current methods for screening aptamers generally require that multiple filter-binding assays be carried out in series and are slow and cumbersome. Bead-based immobilization of aptamers in the context of the electronic tongue may therefore provide an opportunity to screen large numbers of variants in parallel for relative binding to target (and nontarget) ligands.

To evaluate the use of the electronic tongue for aptamer screening, we utilized nine different anti-lysozyme aptamers (denoted as 1−6, E, J, and M in Figure 2A) that had previously been selected from several different random sequence populations.[34] The anti-lysozyme aptamers were transcribed in parallel with biotin-GpG, purified, and immobilized on streptavidin agarose beads. As a negative control, unselected pool RNA similarly conjugated to beads (denoted as "0" in Figure 2A) shows little background binding to lysozyme. Unmodified streptavidin agarose beads (denoted as SA in Figure 2A), as well as beads labeled with an anti-Rev aptamer (denoted as Rev in Figure 2A), served as additional negative controls. All nine anti-lysozyme aptamer and negative control beads were loaded onto a single 4 × 3 chip for screening (Figure 2A). The chip was incubated with fluorescently labeled lysozyme, and the relative amounts of captured fluorescence were determined (Figure 2B, C). Clones 1, 3, and 6 appeared to bind most tightly to the labeled lysozyme. Looking at the image carefully (Figure 2B), there are four additional images surrounding the bead itself (especially for beads denoted as "1" and "6"). As previously discussed,[26] each well is a pyramidal pit whose side is angled inward at 54.7°. This pyramidal shape causes the observed reflections when the bead is observed from the top (as opposed to configurations[26,29,30] in which the flow cell with the chip sits atop an optical/fluorescence microscope). Fluorescent signals were collected only from the center circle, which corresponds to the actual bead, and signals were normalized based on the bead's diameter.

The anti-lysozyme aptamers were then split into three groups, based on their apparent affinities. Three new 4 × 3 chips were loaded with anti-lysozyme aptamers. The three clones which showed the best responsivities (clones 1, 3, and 6) were loaded in triplicate on one chip, while the other six clones were divided into two groups of three (clones 2, 4, 5 and clones M, J, E) and loaded in triplicate on the other two chips. In addition, a negative control (the nascent RNA pool) was loaded in triplicate on each chip. Following the introduction of fluorescent lysozyme, the fluorescence of individual wells was monitored, and the data for each aptamer was averaged.

The binding abilities of the two best anti-lysozyme aptamers (clones 1 and 6) and one aptamer (clone 3) that gave a relatively small signal were further assessed as a function of time (Figure 3). After an initial incubation of 2 min, the beads were washed with 0.4 mL/min of buffer for 28 min (11.2 mL of buffer). Right after the sample incubation, all beads including negative control beads exhibited very bright fluorescence intensity due to nonspecific binding. This nonspecific signal dramatically decreased with washing (compare left and right columns, Figure 3A). The fluorescence intensity of the negative control beads fell to a basal line during the first 10 min of washing (data not shown), while the fluorescence intensity of the aptamer-labeled beads decreased slowly depending on each clone's binding affinity as summarized in Figure 3B. Clone 1 bound approximately 1.1-fold more fluorescently labeled lysozyme than clone 6 and 7-fold more than clone 3 after 10 min of washing. At the end of the buffer wash, clones 1 and 6 exhibited a slight decrease (1.2-fold) in bound fluorescently labeled lysozyme, while clone 3 showed a greater decrease (3.3-fold). This qualitative comparison of dissociation rate con-

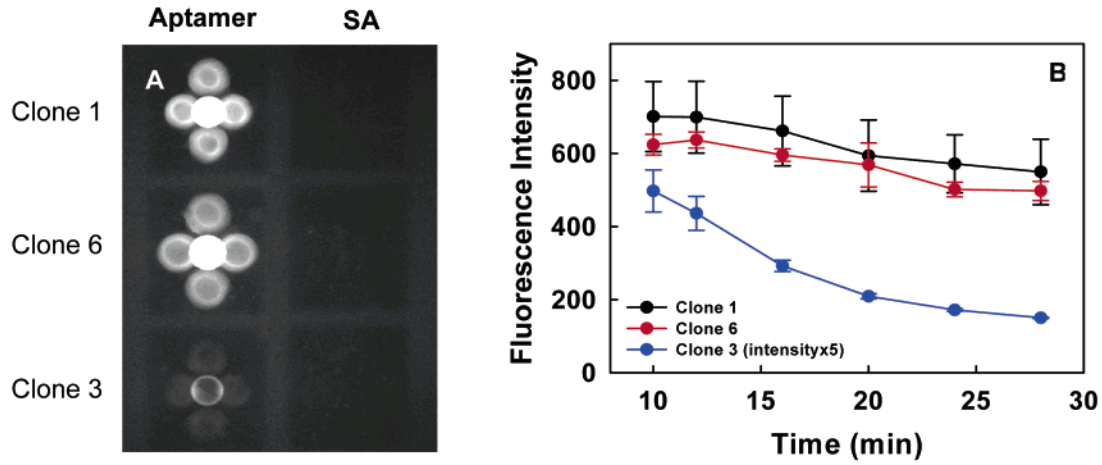

Figure 3. Reactivity of anti-lysozyme aptamers. (A) Fluorescent image of three anti-lysozyme aptamer clones (clones 1, 3, and 6; left column, denoted as "Aptamer") and three negative control beads (right column, denoted as SA) after exposure to Cy3-labeled lysozyme. The image was taken after the clones had been washed for 28 min with Tris buffer. (B) Fluorescence data showing the reactivity of the three anti-lysozyme aptamer clones after 10 min of washing. Images were captured at 10, 12, 16, 20, 24, and 28 min during the washing cycle. Intensity data for individual beads was first corrected by subtracting the fluorescence intensity of the mean of several control beads. Each data point represents the corrected mean fluorescence intensity for three experimental beads ± the standard deviation.

stants confirmed the original rank-ordering of the clones. However, much less aptamer was lost over time based on calculated off-rates than was expected. The retention of fluorescently labeled lysozyme on the beads was likely due to analyte-trapping by the highly concentrated biosensor; once the protein was released from one aptamer, it was quickly bound by an adjacent aptamer. However, while proteins may be partially trapped by interactions with concentrated biosensors, they are not held irreversibly. After stripping the chips with a chaotrope (urea), the fluorescent signal fell to background levels and all three anti-lysozyme aptamer clones once again responded to the reintroduction of fluorescently labeled lysozyme.

Based on these results, we predicted that clones 1 and 6 were the best binding species, with clone 3 having a lesser affinity for lysozyme. To confirm the results obtained with immobilized aptamers on the ET, filter-binding curves were obtained for all of the anti-lysozyme aptamer clones by incubating a constant concentration of radiolabeled anti-lysozyme aptamer with increasing concentrations of lysozyme. The solution-phase binding curves were plotted and used to derive K_d values for each aptamer−lysozyme complex. Clones 1, 3, and 6 had calculated K_d values of 29 ± 5 nM, 83 ± 6 nM, and 128 ± 9 nM, respectively, while the other six clones were well above 230 nM (data not shown).

As can be discerned from the solution-phase K_d values, the results with the immobilized aptamers were not identical. For the solution-phase aptamers, the apparent order of affinity was clone 1 > clone 3 > clone 6, while for the immobilized aptamers the order was clone 1 > clone 6 > clone 3. The differences in the relative affinities of the anti-lysozyme aptamer clones could potentially be due to the fact that solution-phase aptamers were probed with unlabeled protein, while the immobilized aptamers were probed with fluorescently labeled protein.

The effect of aptamer and protein derivatization on measured binding affinities were further explored through a series of additional solution-phase binding assays with clones 1, 3, and 6. In these assays, RNA was either biotinylated or not, and lysozyme was either labeled with Cy3 or not. Biotinylation was found to slightly decrease the aptamers' ability to bind unlabeled lysozyme (data not shown). However, labeling the protein resulted in far less lysozyme being bound by the aptamers, and the relative order of affinities changed, with clone 3 being more sensitive to fluorescent labeling of lysozyme than clone 6. As a negative control, naïve pool RNA (labeled and unlabeled) showed no significant binding to either labeled or unlabeled lysozyme.

Although there are subtle differences between the affinities of suboptimal binders measured on the electronic tongue and those measured in solution assays, the electronic tongue nonetheless provided a quick method for screening the best clones from a selection experiment. Moreover, to the extent that aptamers selected against unmodified proteins are eventually to be used with labeled proteins (for example, in the context of the electronic tongue), the screen provides for the immediate identification of those variants that will have the best analytical performance.

Assay Formats for Arrayed Aptamers. Beyond using the electronic tongue to functionally screen aptamers, it should be possible to use this biosensor array to quantify protein concentrations. In particular, we will demonstrate both the quantitation of labeled proteins, using aptamers as capture reagents (Figure 4A), and the quantitation of unlabeled proteins, in a sandwich assay format with antibodies (Figure 4B).

Quantitation assays were carried out with an aptamer originally selected to bind to the biothreat agent ricin.[35] As before, the aptamer was biotinylated, immobilized, and probed with fluorescently labeled protein (Figure 5). Images of beads with no aptamer (negative control, SA) and beads loaded with anti-ricin aptamer (Aptamer) are shown before (Figure 5A) and after (Figure 5B) injection of the fluorescently labeled ricin. As with lysozyme, the ability of the immobilized aptamer to capture its protein target was manifest.

The fluorescence intensities of the captured proteins could be extracted from these images, and the dose−response curve was generated by plotting the mean fluorescence intensity ± standard deviation (SD) for three independent beads (Figure 5C). One of the advantages of the array format is that data could be collected in parallel, as well as serially. A four-parameter Gompertz equation (SigmaPlot, SPSS, Chicago, IL) was used to plot the best line

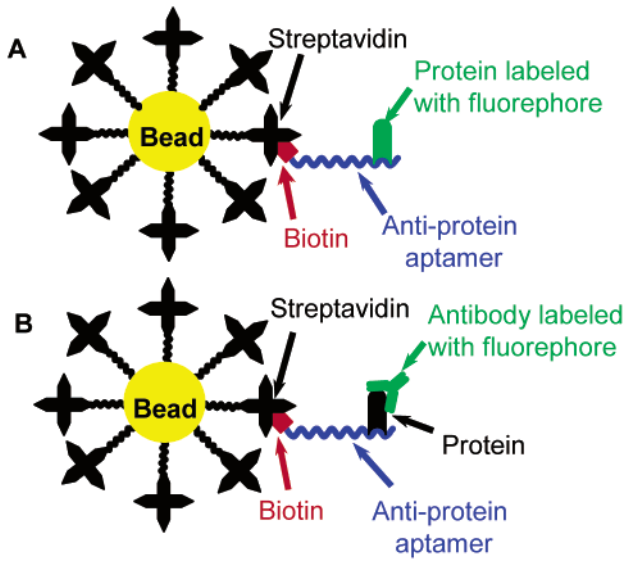

Figure 4. Aptamer assays. (A) Schematic representation of an anti-protein aptamer (immobilized on a streptavidin agarose bead) capturing a fluorescently labeled protein. (B) Schematic representation of an anti-protein aptamer/protein/anti-protein antibody sandwich assay.

through the data points. The calculated detection limit (concentration corresponding to 3 SD above the mean of the background) was slightly lower than 100 pmol of applied sample (8 μg/mL in a volume of 400 μL). The estimated K_d of the aptamer−protein complex was 1.24 μM, which was considerably higher than the reported K_d (7.4 nM).[35] There are several possible reasons for this observed difference. In addition to the disruption of binding due to labeling, immobilization of the aptamers onto beads may have affected the binding affinity by causing steric hindrance or other surface effects.[18,19] The addition of a linker between the aptamer and biotin may alleviate these effects, as McCauley et al. have previously demonstrated.[19] Slow sample penetration into the porous beads could also have led to a decrease in the observed affinity. According to recent confocal analyses,[32] sample access was restricted in the lower half of beads due to interactions with the walls of the pyramidal pits, and this was thought to operationally decrease the detection of molecular interactions. However, since the sample was pumped through the beads under pressure over a period of several minutes, it seems likely that the receptors would have had adequate time to equilibrate.

In order to examine whether unlabeled ricin could also be detected, a sandwich assay format as shown in Figure 4B was adopted. In this system, anti-ricin aptamer acted as a capture reagent and unlabeled ricin served as a bridge to a fluorophore-labeled antibody that served as a reporter. Although it was not known in advance whether the aptamer and antibody would compete for the same epitope on ricin, a fluorescent signal was readily obtained when all of the components of the sandwich were in place. A negative control that lacked ricin yielded no fluorescent signal (Figure 5D). By employing this sandwich format we could detect as little as 1 pmol of unlabeled ricin (320 ng/mL in a volume of 100 μL).

The general problem of using modified proteins with reagents selected to bind to unmodified proteins could potentially be solved through the use of sandwich assays, as described above. In addition, it should be relatively simple to adapt in vitro selection procedures to select for aptamers that will bind to protein targets that have previously been modified with the same dye or other conjugate that will be used during detection.

Because of the unexpected influence of analyte modification on affinity, experiments were also performed to ensure that the solution-phase selectivity of the aptamers remained intact following immobilization. Two different aptamers, the anti-ricin aptamer and

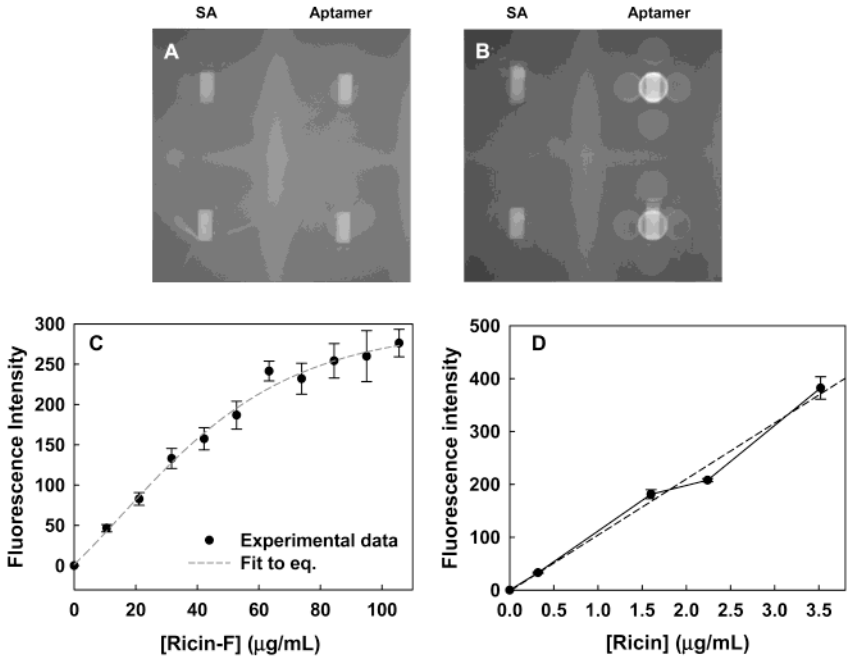

Figure 5. Response of anti-ricin aptamer. (A) Background of control streptavidin agarose beads (denoted as SA) and anti-ricin aptamer beads (denoted as Aptamer). (B) Aptamer response after the addition of Alexa-Fluor$_{488}$-labeled ricin. (C) Quantitation of Alexa-Fluor$_{488}$-labeled ricin with anti-ricin aptamer beads. (D) Quantitation of unlabeled ricin via an anti-ricin aptamer/ricin/anti-ricin antibody sandwich assay. Intensity data for individual beads was first corrected by subtracting the mean fluorescence intensity of several negative control beads. Each data point represents the corrected mean fluorescence intensity for five experimental beads ± the standard deviation.

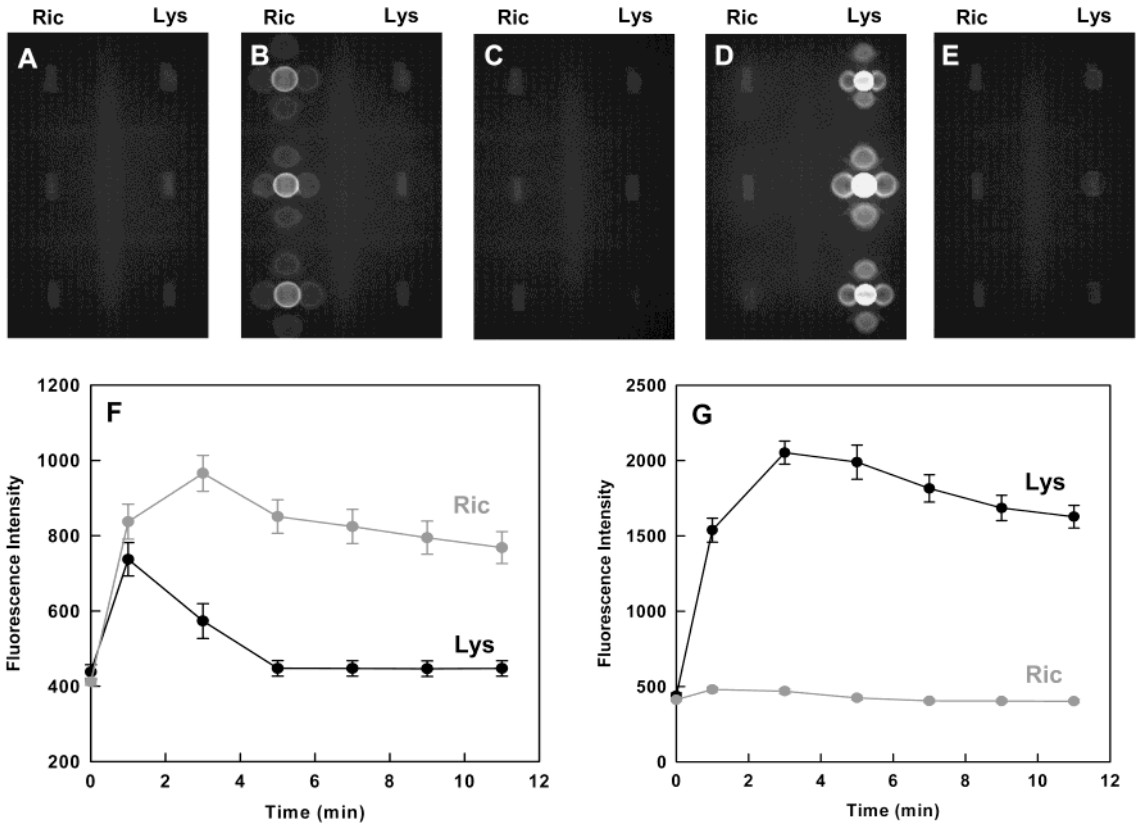

Figure 6. Selective responses of anti-ricin aptamer and anti-lysozyme aptamer. (A) Background of anti-ricin aptamer beads (denoted as Ric) and anti-lysozyme aptamer beads (denoted as Lys). (B) Aptamer response after the addition of Alexa-Fluor$_{488}$-labeled ricin. (C) Removal of bound protein from aptamer beads (aptamer reactivation). (D) Aptamer response after the addition of Alexa-Fluor$_{488}$-labeled lysozyme. (E) Removal of bound protein from aptamer beads (aptamer reactivation). (F) Fluorescence intensity of the aptamer beads after exposure to Alexa-Fluor$_{488}$-labeled ricin. (G) Fluorescence intensity of the aptamer beads after exposure to Alexa-Fluor$_{488}$-labeled lysozyme. Each data point represents the mean fluorescence intensity ± standard deviation for three beads.

anti-lysozyme aptamer (clone 1) were assayed on a single 3 × 2 chip. Initial background images were captured prior to protein incubation (Figure 6A, and $t = 0$ in Figure 6F). The beads were incubated with fluorescently labeled ricin in PBSM for 1 min ($t =$ 1 min in Figure 6F), and then washed with PBSM for 10 min in order to remove any nonspecifically bound protein. Upon the addition of Alexa-Fluor$_{488}$-labeled ricin, an increase in fluorescence intensity was seen for both sets of aptamer beads. However, following the wash step the anti-lysozyme aptamer beads (clone 1) returned to background levels of fluorescence (Figure 6F). Images showing the aptamer beads' response to the addition of fluorescently labeled protein (captured after the 10 min PBSM buffer wash) were acquired (Figure 6B). The aptamer beads were washed with an elution buffer after each protein incubation to verify that the fluorescently labeled proteins could be removed. Signals equivalent to the initial background level were generated (Figure 6C, and $t = 0$ in Figure 6G). The process was then repeated with the addition of fluorescently labeled lysozyme, rather than fluorescently labeled ricin (Figure 6D, E, and G). Fluorescence data were again collected as a function of time. Conversely, the anti-ricin aptamer beads showed no appreciable increase in fluorescence intensity upon the addition of the Alexa-Fluor$_{488}$-labeled lysozyme (Figure 6G). Lysozyme is a particularly good control in this regard, as it is very basic (p$I = 9.1$) and is known to bind nonspecifically to nucleic acids. Overall, while there may be some nonspecific binding of labeled proteins to aptamers, specificity is ultimately obtained by simply washing the beads.

Aptamers can be directly compared with antibodies as capture reagents. Ligler and co-workers[40−4340−43] could detect ricin concentrations as low as 8 ng/mL[40] by employing an antibody-based immunosensor array, in which biotinylated capture antibodies were immobilized onto avidin-coated microscope slides, and sandwich assays were carried out with ricin and a fluorescently labeled antibody. It is instructive that aptamers have detection limits and performance characteristics that are similar to those previously exhibited by antibodies. The initial success of the sandwich assay and the fact that beads are contained within microwells on the electronic tongue format also raises the possibility that enzyme-linked immunoassays can be carried out to boost signals and lower detection limits.

Reusable Biosensors. The development of a chip array that could be used for repetitive or continuous analyte monitoring would be extremely useful. However, antibodies and other protein-based biosensors cannot generally be used more than once. Once a protein has captured or interacted with an analyte, the analyte must be stripped from the protein under conditions that frequently also denature the protein. Because of this, most protein-based biosensors or chip arrays are used only once, then discarded.

(40) Ligler, F. S.; Taitt, C. R.; Shriver-Lake, L. C.; Sapsford, K. E.; Shubin, Y.; Golden, J. P. *Anal. Bioanal. Chem.* 2003, *377*, 469−477.
(41) Delehanty, J. B.; Ligler, F. S. *Anal. Chem.* 2002, *74*, 5681−5687.
(42) Taitt, C. R.; Anderson, G. P.; Lingerfelt, B. M.; Feldstein, M. J.; Ligler, F. S. *Anal. Chem.* 2002, *74*, 6114−6120.
(43) Rowe-Taitt, C. A.; Golden, J. P.; Feldstein, M. J.; Cras, J. J.; Hoffman, K. E.; Ligler, F. S. *Biosens. Bioelectron.* 2000, *14*, 785−794.

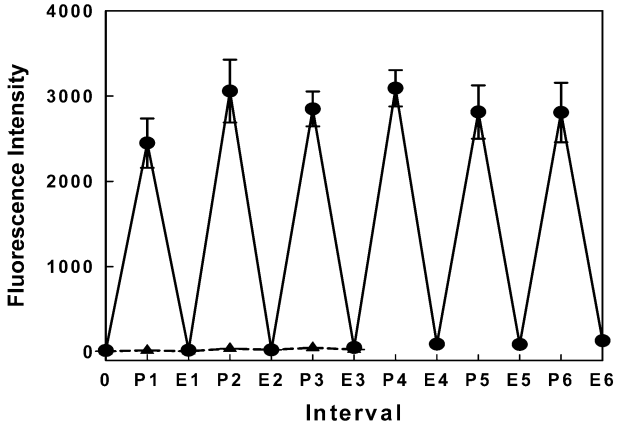

Figure 7. Reactivation of anti-ricin aptamer beads. Fluorescence measurements of anti-ricin aptamer beads (circles) were taken at 13 different intervals. Fluorescence measurements of pool RNA beads (triangles) were taken at seven different intervals. Interval 0 records the background fluorescence of unexposed anti-ricin aptamer and pool RNA beads. Intervals P1−P6 show the fluorescence intensity of the anti-ricin aptamer beads upon binding an Alexa-Fluor$_{488}$-labeled ricin. Intervals P1−P3 also show the fluorescence intensity of the pool RNA beads upon binding Alexa-Fluor$_{488}$-labeled ricin. Intervals E1−E6 show a drop in fluorescence (down to the background level) consistent with the denaturing and reactivation of the anti-ricin aptamer beads. Intervals E1−E3 also show the fluorescence intensity of the denatured pool RNA beads. Each data point (for every interval in the sequence) represents the mean fluorescent intensity ± standard deviation for five beads.

In contrast, aptamers can frequently be denatured and refolded multiple times without loss of activity, in part because the aptamer binding function is largely dependent upon simple, stable secondary structural interactions, rather than more complex, weaker tertiary structural interactions, as in proteins. The primacy of secondary structure in aptamer binding function also means that aptamers can be readily engineered for additional stability by adding base-pairs to stem structures. Moreover, since aptamers are typically denatured and refolded during each successive round of in vitro selection, they have to some extent been "pre-evolved" for reusability.

All of these considerations suggested that the aptamer chip arrays that we had produced might be reusable. In order to test the structural robustness of aptamers, aptamer-labeled beads were treated by either heating to 3 min at 70 °C, by washing with a buffer containing 7 M urea, or by both heating and washing. After each treatment, beads were incubated with Alexa-Fluor$_{488}$-labeled ricin, washed, and the amount of captured protein was determined by fluorescence microscopy. There was no drop in the efficiency of protein capture compared with no treatment.

In order to demonstrate that aptamer chips could in fact be reused multiple times, we carried out an assay similar to the one shown in Figure 4A, but between each assay captured ricin was eluted from the aptamer with a buffer containing a high concentration of urea. This buffer was exchanged for the normal binding buffer, the aptamers were allowed to refold, and ricin was reintroduced into the buffer stream (Figure 7) In greater detail, initial background fluorescent images were taken of anti-ricin aptamer beads and pool RNA beads (Figure 7, interval 0). The anti-ricin aptamer beads were then incubated with Alexa-Fluor$_{488}$-labeled ricin (Figure 7, interval P1; circles), followed by an elution buffer wash (Figure 7, interval E1; circles). In parallel, pool RNA beads were incubated with Alexa-Fluor$_{488}$-labeled ricin (Figure 7, interval P1; triangles), followed by an elution buffer wash (Figure 7, interval E1; triangles). Five more incubation/elution cycles were performed with the anti-ricin aptamer beads (Figure 7, intervals P2−P6 and E2−E6; circles), and two more cycles were performed with the pool RNA beads (Figure 7, intervals P2−P3 and E2−E3; triangles).

It is interesting to note that the fluorescence intensity signal from the initial protein exposure (P1) for the anti-ricin aptamer beads is slightly lower than the signal generated from all five subsequent protein incubations. These results are consistent with the notion that aptamers must undergo denaturation and refolding steps similar to those that were present during their initial selection in order to attain full activity. As a further confirmation of this observation, immobilized aptamers that were initially heat-denatured were able to capture more analyte than immobilized aptamers that did not see such a heat denaturation step (data not shown).

CONCLUSIONS

Aptamers are potentially useful biosensor reagents that can both substitute for antibodies and that can be adapted in novel ways to sensor platforms. However, methods must be developed to adapt aptamers to sensor arrays. To this end, a facile method for aptamer conjugation to a bead-based sensor array, the electronic tongue, was developed. The immobilized aptamers could specifically capture protein analytes, and aptamer chips were used to identify the best aptamers from in vitro selection experiments.

Assays for protein identification and quantitation were developed and applied to the detection of the biothreat agent ricin. The limits of detection (320 ng/mL) in a sandwich assay format were comparable to those previously observed with antibody assays. However, unlike antibody assays, the aptamer arrays could be completely stripped of protein analyte and reused without loss of function. These results raise the prospect that aptamers could be adapted to function as reusable, long-term biosensors in arrays.

ACKNOWLEDGMENT

This research was supported by the Arnold and Mabel Beckman Foundation, Office of Naval Research (N00014-00-1-0930), Department of the Army Research, MURI (DAAD19-99-1-0207), National Science Foundation (EIA-0219447), and the Countermeasures to Biological and Chemical Threats Program at the Institute for Advanced Technology (DAAD13-02-C-0079; UTA03-0203).

Received for review January 23, 2004. Accepted April 22, 2004.

AC049858N